IJSCET

International Journal of Sustainable Construction Engineering and Technology

Damage Parameter Variations of Breakwater Along with a Floating Wave Barrier and a Submerged Obstacle

Ramin Vafaeipour Sorkhabi[1], Alireza Naseri[1*], Mohammad Taghi Alami[2], Alireza Mojtahedi[2]

[1]Department of Civil Engineering, Tabriz Branch
 Islamic Azad University, Tabriz, IRAN

[2]Department of Water Recourses Management, Faculty of Civil Engineering,
 University of Tabriz, Tabriz, IRAN

*Corresponding Author

Abstract: Damage to rubble mound breakwaters (RMBs), both general and partial, causes instability and inconstancy of the structure against waves. This study aimed to investigate the effect of a submerged obstacle on the stability and damage reduction of RMBs as an innovative method and determine the optimal distance of the obstacle from the breakwater and the floating wave barrier based on the damage parameter. The waves affecting the breakwater were assumed to be random using a JONSWAP spectrum. The aggregates' movement and the RMB's exact deformation were recorded using close-range photogrammetric imaging, and the eroded area and the damage parameters were obtained at equal distances in eight cross-sections. According to the results of the tests, by analyzing the effect of the number of waves hitting the breakwater, 3000 waves were considered to bring the structure to a stable state. The results showed that increasing the relative wave height from 0.36 to 0.48 and from 0.48 to 0.6 increased the damage parameters to 39.12% and 44.44%, respectively, and increasing the relative wave period from 0.6 to 0.8 and 0.8 to 1 increased the damage parameters to 22.94% and 28.26%, respectively. Moreover, using a seaward obstacle at 0, 5, 10, 15, and 20 cm distances decreased the damage parameter. The greatest effect, a reduction of 39.15% in the damage parameter, was observed at a distance of 5 cm from the RMB. This number was reduced to 0.735 when a floating wave barrier was used without a submerged obstacle (i.e., 34.14%). Using an obstacle at 5 cm in conjunction with a wave barrier reduced the damage parameter by 54.03% and demonstrated the best function among different models. Hence, this model is proposed based on the experiments carried out in this study.

Keywords: Rubble mound breakwater, damage parameter, submerged obstacle, floating wave barrier, random wave

1. Introduction

Rubble mound breakwaters (RMBs) are used to dissipate sea wave energy and protect facilities and shoreline areas from damage. These structures are typically composed of three major layers: core, filter, and armor (Khosravi Babadi et al., 2017). It has been attempted to reduce the hydrodynamic forces caused by waves by reshaping and launching RMBs to create a stable structure profile (Ghanbarian, 2010). Researchers have been conducted numerous tests on the stability of the armor layer and the effect of structural and hydraulic parameters on the RMBs damage. Da Silva et al. (2016) investigated the relationship between structural features such as wall slope, crest width, breakwater height, and attacking wave performance. Lamberti et al. (1994) emphasized the importance of water depth at the structure's base and shallow

water conditions in their modeling. They demonstrated that the final profile deformation coefficients were related to reflection depth, wave sharpness, and floor slope in addition to wave height. The reduction of wave forces as the radius of curvature of the structure increased was notable in this study. In another experimental study, it was shown that the wave height parameter H_{50}, defined as the average wave height of the 50 highest waves reaching an RMB in its useful life, can describe the effect of the wave height on the history of the armor damage caused by the wave climate during the structure's usable life. Also, it was shown that the current sea-state stability formulae for RMBs can be easily modified to use the wave height parameter H_{50}. After analyzing the experimental results, it was shown how H_{50} formulae can predict the observed damage independently of the sea state wave height distribution or the succession of sea states (Vidal et al., 2006). By examining the stability of RMBs in terms of breaking similarity parameter, Sayao (1998) evaluated the permeability of the structure as an essential factor in the hydraulic stability of the structure.

Also, the dimensions of the rocks used in breakwaters are related to the armor damage level in the face of the waves. Rao and Pramod (2003) demonstrated in experiments that as the size of the rocks decreases, the amount of damage to them increases. The stability of rock slopes with a horizontal berm was studied by van Gent (2013), focusing on the slope above the berm and the slope below the berm. He derived prediction formulae based on the test results to quantify the required rock size for rubble mound breakwaters with a berm. The results of the Experiments showed that: the rock size in the upper slope, i.e., the slope above the berm, can be significantly smaller than for a straight slope without a berm; the influence of a berm is more significant in combination with a steep slope than in combination with a gentle slope; for the submerged berms, the reduction in damage levels to the lower slope depends on the level of the berm and the width of the berm; finally, because the damage occurs at the seaward side of the berm, landward of the position at the berm where the damage ends, a smaller rock size may be applied. In another study, Galiatsatou et al. (2018) determined that the most common cause of failure of conventional RMBs was damage to the armor layer, scouring of the structural toe, or upward and overflow of waves. Celli et al. (2019) evaluated in a project how submerged berms configuration influences the seabed soil response and momentary liquefaction occurrences around and beneath breakwaters foundation, under dynamic wave loading. They assessed the effects of submerged berms on the incident wave's transformation using a phase resolving numerical model for simulating non-hydrostatic, free-surface, rotational flows. They performed this assessment by a parametric study by varying the berm configuration (i.e., its height and length), keeping the offshore regular wave condition constant, the berm and armor layer porosity values, the water depth, and the elastic properties of the soil. Results indicated that submerged berms tend to mitigate the liquefaction probability than straight sloped conventional breakwater without a berm. In addition, it seemed that the momentary liquefaction phenomena are more influenced by changing the berm length rather than the berm height. Also, van Gent and van der Werf in 2014 examined Rock toe stability of RMBs. They have studied rock toe stability through physical model tests to determine the required rock size in the toe structure. Their analysis was focused not only on the influence of the wave height and the water depth above the toe structure but also on the influence of the width of the toe structure, the thickness of the toe, and the wave steepness. The results showed that the wave steepness, width of the toe, and the thickness of the toe affect the damage to the toe; these parameters need to be taken into account to derive accurate predictions of the damage to the toe structure. Based on these research results, a prediction formula has been derived, including these effects, which can be used to determine the required rock size in the toe of rubble mound breakwaters within the ranges of the performed tests. The effects of submerged berms on the stability of RMBs were studied by Celli et al. (2018). Their research aimed to provide a new design criterion for the armor layer of conventional breakwaters with submerged berms marked by small thickness compared to water depth. They proposed a new design criterion able to describe the influence of relatively low and long berms on the stability of the armor of conventional breakwaters. Their proposed method is valid for deep and shallow waters and easy to use as it is almost similar to standard criteria with the needing for the further estimation of the correction factor depending upon the berm configuration (i.e., length and water depth) and the incident wave length at the toe of the structures evaluated by using the peak period.

It is also essential to brief review the performance of submerged breakwaters due to the use of submerged obstacle in the present research experiments. One of the solutions to coastal erosion is the use of submerged breakwaters (Padashi and Tajziyehchi, 2010; Chegini, 2010). Wave breaking by submerged breakwaters causes turbulence at the RMB's toe. Friction resistance and turbulence increase energy dissipation by reducing wave reflection and bed scouring, thereby adjusting sediments (Khosravi Babadi et al., 2017). According to the findings of Neves et al. (2007), the permeability of submerged breakwaters influences the flow characteristics caused by waves and reduces horizontal flow velocity. It is also possible to reduce wave energy by applying submerged obstacles. Bungin (2021) used a set of 5 cm cubes with a distance of 1.1 cm in a 100 and 200 cm path as a submerged breakwater in a laboratory study and observed that wave height decreased by 60-80%. Hao et al. (2019) used the fluid-structure interaction (FSI) algorithm to numerically model submerged breakwaters in one and two rows in the face of regular waves. They evaluated the effectiveness of the second row of breakwaters as favorable. In addition to protecting the existing breakwater, submerged breakwaters protect shorelines and the facilities. These structures are used to reconstruct RMBs that have been damaged or destroyed (Juhl and Jensen, 1995). Tulsi and Phelp (2009) investigated the effect of a submerged breakwater on protecting the crown of a damaged RMB. They discovered that the submerged structure could break and weaken storm waves, save the damaged portion of the RMB, and eventually repair the main RMB. Given the behavior of the submerged obstacle, it appears appropriate to use it as a structure alongside the RMB. Constructors design this composite structure using precise and

critical information such as wave characteristics and structural properties. It is thought that modifying the dimensions, wall slope, and position of the submerged structure can improve the breakwaters' optimal performance (Smith et al., 1996). Stefanutti Stocks (2015) reduced the weight characteristics of the breakwater armor layer in a project by designing a set of submerged breakwaters to reduce waves and protect the RMB near the coast. Furthermore, Cox and Clark (1992) constructed a reinforced RMB made of submerged reef that was placed a short distance in front of the main structure, a project that yielded promising results. The dual combining and reinforcing role of the structure improved the function while reducing stones consumption. It was discovered that the height of the main structure could be reduced by 1.5 m, resulting in significant cost savings.

RMB damage indicates structural demolition and hydraulic instability in the face of the waves (Mousavi, 2010). Thus, modeling the damage progression and investigating the representative parameters of this process in order to improve the function and lifespan of the breakwater appears to be critical. In this process, selecting new methods and critical variables to reduce the number of experiments without affecting the results in estimating breakwater damage levels has been considered by researchers. Janardhan et al. (2015) used a variety of methods, including PCR. Noting the complexity of the progression of damage in the Armor layer due to the random nature of the impact of the waves. Campos et al. (2020) considered accurate imaging techniques to monitor the structure's function very useful and essential.

By examining various references, this research has been conducted as an innovative method in the form of an experimental study where used the damage parameter to explore the effects of a submerged obstacle and a floating wave barrier in front of an RMB. Therefore, the submerged obstacle was connected to the structure (at various distances), and the floating wave barrier was placed 50 cm away. Under the influence of random waves, the damage number was obtained and compared. To increase the accuracy for recording the breakwater deformation and damage and reduce the repetition of experiments, three-dimensional imaging, and modeling methods were used, described in the following sections.

2. Materials and Methods

The results of various studies on the stability of Reshaping RMBs show that even despite the formation of stable profiles, the possibility of displacement and lateral movement of rocks and dynamic performance may cause crushing and wear of reinforcement rocks and ultimately reduce the stability of the structure (Mostaghiman and Moghim, 2022). Therefore, using a method to reduce damage to the structure and promote breakwater stability can be helpful and practical. A submerged obstacle acts as an RMB berm during reshaping by supporting and reducing rock fall, allowing a stable breakwater configuration to form on a smaller range. The distance of the obstacle from the toe and its effects on the damage parameter is critical for determining stability. Due to rock fall, the obstacle becomes part of the breakwater body when the distance is too short. However, when it is too large, the spacing undermines the effectiveness of the obstacle's role as a support. Accordingly, the distance is an essential parameter for minimizing the damage parameter as a measure of stability. A floating wave barrier can also help control the damage done to the RMB by lowering the wave's height and energy. Using an optimally spaced submerged barrier in conjunction with a floating wave barrier can significantly reduce wave energy and the amount of damage to the RMB.

2.1 Test Procedure

The present study investigates experimentally how the position of a submerged obstacle affects the stability of an RMB at different (seaward) distances. During the model experiment, the position of the submerged obstacle was changed, and the effects on the RMB's damage parameter were investigated. In addition, the impact of a floating wave barrier in front of the RMB was examined. To this end, the breakwater was tested three modes: once without the submerged obstacle, once with the obstacle at 5 cm intervals 0-20 cm from the RMB, and once with both the obstacle and the wave barrier simultaneously, all under similar conditions; the damage parameter was calculated and compared in each case. In this study, the submerged obstacle is referred to as an obstacle, and the floating wave barrier, which is placed 50 cm away from the RMB, is referred to as the wave barrier. According to the introduction, RBM stability has primarily been studied in the structure's lateral or middle sections.

On the other hand, the present study used close-range photogrammetric imaging to provide dense cloud and a combined integrated 3D model of various height elevations to develop a detailed RMB model before and after the wave attacks. The images taken from a close distance were analyzed in close-range photogrammetric imaging to obtain a reshaped RMB model that could pinpoint the displacement at any point accurately. Since the RMB profile upon encounter with waves did not follow a regular change trend along with the structure, and it constantly changed, some unforeseen changes occurred. This issue complicates studies. Well-documented and accurate data leads to better research results, contributing to the precise measurement of the RMB displacement of armor rocks when they come into contact with waves. This method is non-destructive and has no negative consequences, and it provides real-time 3D measurements with increased accuracy and speed. Furthermore, the waves generated by the wave maker were based on the JONSWAP spectrum ($\gamma = 3.3$), which was selected because of its high spectral energy and can be one of the most appropriate spectra for laboratory studies in the absence of a field spectrum.

Tables 1 and 2 list various governing variables and non-dimensional characteristics used in this study. Wave steepness is the most important factor to consider when determining wave height and period. It is critical to evaluate the

wave height and period to place the wave steepness generated by combining the two parameters in the 0.015-0.07 range (Van der Meer, 1992). In some studies, a combination of wave height and period with a steepness range of 0.01-0.054 has been proposed (Andersen, 2006; Burcharth, 1993). Because it is possible to observe scale effects in waves with less than 4 cm height, the wave height was adjusted in the range between 4 and 15 cm based on the laboratory facilities, depth, and type of wave maker conditions. However, turbulence at the surface of generated waves is expected due to large displacements at the paddle-generated wave, which perplexes the accuracy of the data collected. Also, the non-breaking waves were the only ones investigated in this study.

Table 1 - Range of governing variables

Variable	Expression	Range
Significant wave height [m]	H_s	0.09 to 0.15
Peak wave period [s]	T_p	0.9 to 1.5
Nominal diameter [cm]	D_{n50}	1.7
Mass density [kg/m^3]	ρ	2550
Water depth [m]	d	0.25
Slope angle	α	1:1.25

Table 2 - Non-dimensional characteristics

Variable	Expression	Range
Storm duration	N	3000
Reynolds number	R_e	1.59×10^4 to 2.66×10^4
Ratio of the thickness of armor layer to the nominal diameter	t_A/D_{n50}	15
D_{n85A}/D_{n15A}	f_g	1.82
Wave steepness	s_o	0.026 to 0.078
Relative wave height	H/d	0.36 to 0.60
Relative wave period	T/T_{max}	0.6 to 1

In marine model experiments, gravity is considered the dominant force. Scale effects that occur mainly due to the small values of the Reynolds number and the different hydraulic behavior of the actual model and sample; should be reviewed and evaluated. The flow at the base of the structure must be sufficiently turbulent to minimize the effect of scale and viscosity. The study and control of this effect have been done using Eq. 1 (Van der Meer, 1988).

$$R_e = \frac{\sqrt{gH_s}\, D_{n50}}{\upsilon} \tag{1}$$

Where $\sqrt{gH_s}$ and D_{n50} are the characteristic velocity and length, and υ is the kinematic viscosity. Various studies were carried out on scale effects (Hughes, 1993; Jensen and Klinting, 1983). To minimize the viscous scale effects, according to the recommendations of Van der Meer, the Reynolds number is considered in the range of $10^4 < Re < 4 \times 10^4$. The minimum value of Reynolds number in the performed experiments is 1.59×10^4, and the effect of scale due to viscosity can be ignored.

2.2 Wave Flume and Breakwater Model

The tests were carried out in a 35-meter-long, 5-meter-wide, and 1-meter-deep flume at the Soil Conservation and Watershed Management Research Institute (SCWMRI); its dimensions are depicted in Figs. 1, 2.
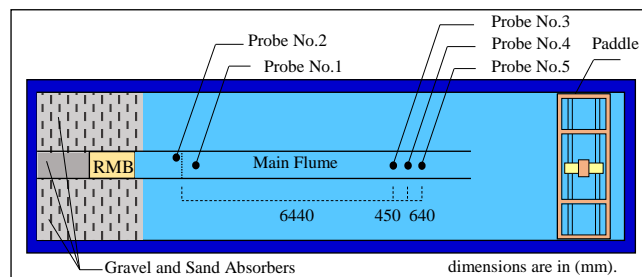

Fig. 1 - Sketch of wave flume and position of the RMB structure and wave probes
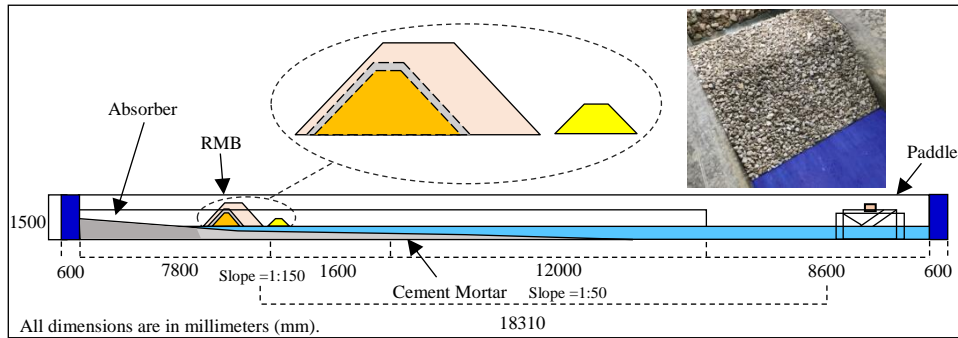
Fig. 2 - Transversal section of the wave flume and the position of the RMB and the obstacle

The breakwater with a uniform slope of 1V:1.25H is constructed on the flatbed of the flume with primary stone armor of nominal diameter D_{n50} equal to 1.7 cm. The chosen geometric scale in this study is 1:50. Plexiglass is used to design a stable obstacle 80 mm in height. The obstacle has a slope of 1V:1.25H and is installed uniformly seaward the RMB. The obstacle is filled with heavy material to submerge and behave more steadily against the waves completely. Furthermore, a 100 mm plexiglass wave barrier is designed; the weight of this barrier is precisely adjusted to submerge in the water to half its depth (with 50% immersion) while being held to the flume bed by a wired cable. The white anti-reflective fabric is used to cover the obstacle to avoid light reflection and imaging errors while capturing the location of points and profiles. Fig. 3 depicts RMB, obstacle, and barrier features, while Fig. 4 depicts their images during the fabrication and experiment phases.
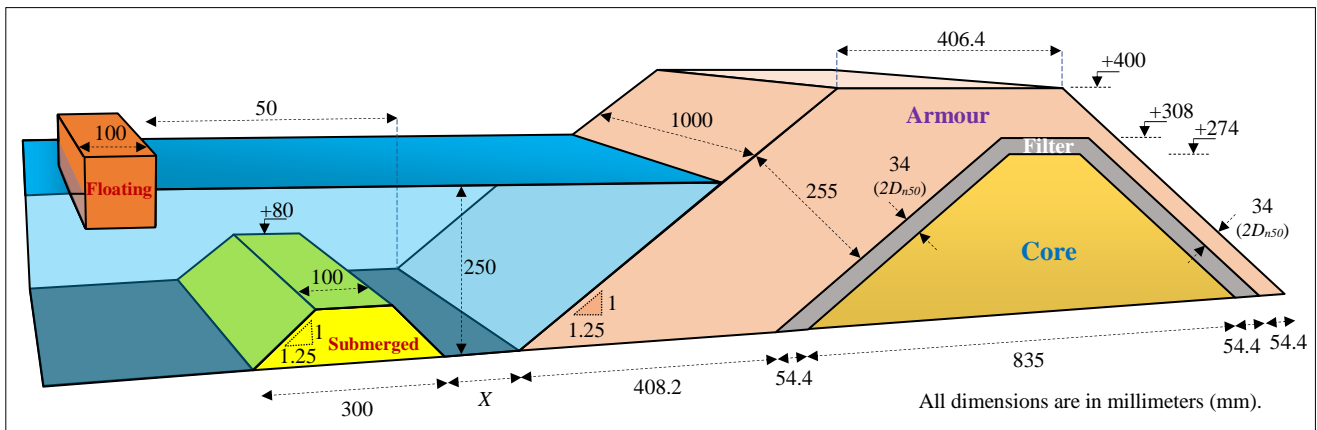

Fig. 3 - Dimensions and distances of the RMB, submerged obstacle, and floating wave barrier

Fig. 4 - Images of RMB layers, submerged obstacle, and floating wave barrier

2.3 Measurements and Data Interpretation

The structural responses and stability of the RMB in the presence of an obstacle and a wave barrier were investigated by analyzing an experimental model both without and with the obstacle placed at 5 cm intervals 0-20 cm from the breakwater. The experimental setup was calibrated and controlled before testing. Some assumptions were also taken into account in the tests, such as the fact that secondary waves in the wave generation process are not considered, the flume bed is horizontal, only the model's hydraulic performance is assessed, and wave reflection from the breakwater does not collide with newly generated waves (Ataie Ashtiani, 2006). 11 points on the flume were first marked by recording the coordinates of the breakwater range with a surveying camera to create the 3D model (Fig. 5). The breakwater was then photographed with a professional camera before and after tests (or after a certain number of waves); images were then transferred to software, processed, and digitized to produce photo blocks. Finally, the Digital Elevation Model (DEM) and Digital Surface Model (DSM) were created. Table 3 lists some of the software-specified properties of the integrated 3D model.

Fig. 5 - Surveying the position of base points and locating markers

Table 3 - Specifications of the 3D model

Aligned Cameras	GCP (Markers)	Dense Point Cloud	Tie Points	Flying Altitude (m)	Coverage Area (m²)
27	11	3488378	26907	1.13	2.28

Images of the structure surface were taken at regular intervals. 25-27 images were prepared for each test segment and transferred to the software to create a 3D model. Fig. 6 shows a sample of markers and photographs taken from the breakwater in the Agisoft. With Agisoft Metashape, very accurate 3D models of camera images can be prepared. It also can produce digital models with high accuracy. Due to the high quality of the images used, the photo scan accurately measures the area and volume. The increased ability to reduce computing time when working with extensive data makes this software an effective and valuable option for working with data and displaying its details (Ebadi and Esmaeili, 2018).
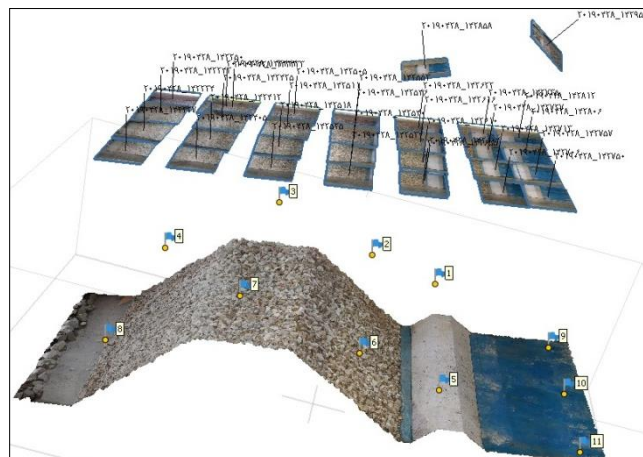

Fig. 6 - Position of markers and cameras from the RMB

The following figures show the model-making process. Fig. 7 shows the model-making process. Fig. 7(a) depicts a set of tie points that can be considered reference points and indicators for model construction due to sharing two or more images. Fig. 7(b) also shows the dense cloud with 3D coordinates and creates the outer surface of the model. According to table 3, more than 26,000 node points and about 3.5 million dense point clouds are defined in these images. Fig. 7(c) also shows the initial model, and Fig. 7(d) shows the final model after adding texture to the surfaces. Fig. 8(a) depicts a set of images taken, while Fig. 8(b) represents image overlaps, and Fig. 8(c) shows the DEM.
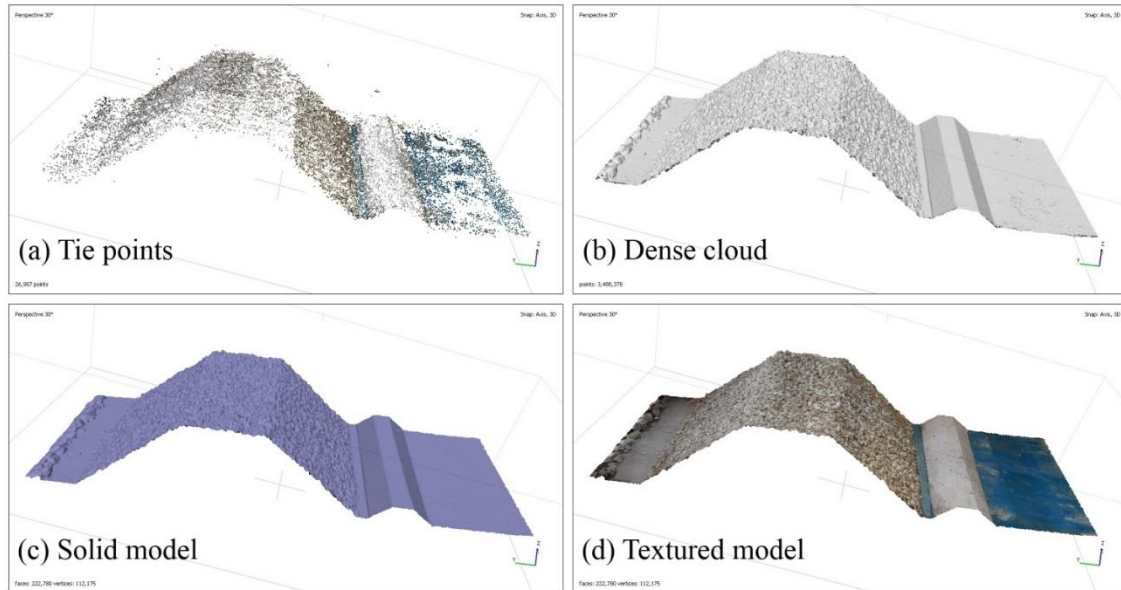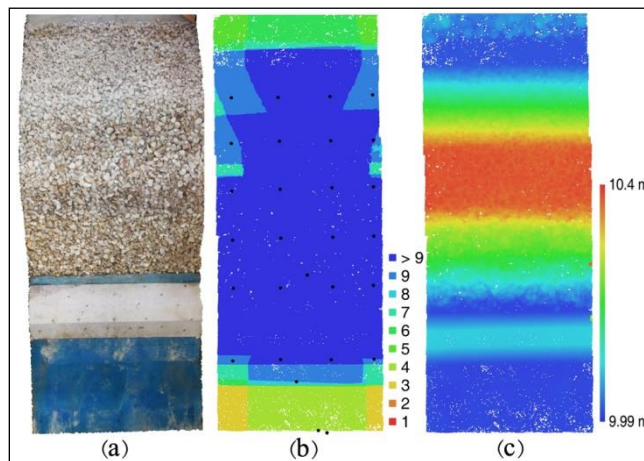

Fig. 7 - 3D model-making process

Fig. 8 - (a) Integrated images; (b) images overlaps; (c) DEM

3. Results and Discussion

Analyzing test results using the main parameters is essential for studying RMB hydraulic stability.

3.1 Wave Analysis

The wave paddle is of the piston type. The wave maker could generate regular and random waves using the Bretschneider, Pierson-Moskowitz, and JONSWAP spectrums, with a maximum height of 20 cm. The wave probes are based on resistance detectors and could accurately measure the water surface fluctuations regarding the static water surface. The wave height was obtained for each solo wave using the time series obtained through the zero up-crossing methods. In this method, the wave intersects the reference line (water surface elevation) in two points. The wave height is the maximum difference of water surface elevation between two solid points and the wave period is the time interval from the first solid point to the second one (Viriyakijja and Chinnarasri, 2015; Vafaeipour Sorkhabi and Naseri, 2019). Accordingly, a MATLAB code was written that used water surface time series to differentiate the waves and provide the heights and periods of the individual waves. The resultant height and periods were used to calculate the maximum height,

significant wave height, average wave height, maximum period, significant wave period, average period, wavelength, and frequency. Fig. 9 depicts the JONSWAP spectrum as well as the experimental spectra. Based on the results, the wave height and period through the zero up-crossing results do not match the observed values. However, the significant mode was closest to the wave maker's height and period between the mean, significant, and maximum wave heights and periods. This can be seen in the JONSWAP spectrum generated by the wave maker at the water's surface and the wave separation code results. For example, given a wave height of 12 cm for the wave maker, the wave heights in mean, significant, and maximum modes were 5.3, 11.38, and 15.59 cm, respectively. This finding was supported by all of the tests that were carried out.
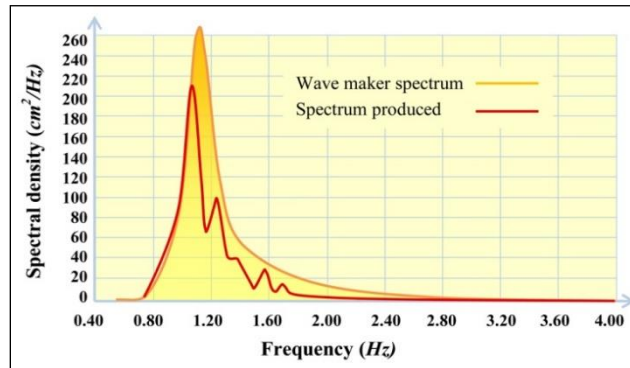

Fig. 9 - JONSWAP spectrum and experimental spectra

Consequently, the wave maker's height and period can be approximated as the significant height and period. The number of waves generated by the water surface was also less than expected. For example, at a wave height of 12 cm, a period of 1 second, and a duration of 5400 seconds (1.5 hours), 5400 single waves were expected, whereas the zero up-crossing method generated 5173 waves. The water surface transfers to the next wave without cutting the zero level in tiny waves, causing this reduction. In counting the waves, that wave is almost completely eliminated. According to tests, the discrepancy between these two numbers regarding the effect of the number of waves on the RMB reshaping was insignificant as it was controlled for experiments.

3.2 Waves Effect Analysis on RMB Reshaping and Damage

RMB (as the control test) was subjected to random waves at the start of the experiments to accurately observe the function of the obstacle and the wave barrier. Furthermore, the reshaping of armor at various heights and periods was investigated so that the controlled structure against the waves could determine the damage to the RMB realistically and accurately. By the damage parameter, it is meant:

$$S = \frac{A_e}{D_{n50}^2}$$

(2)

Where A_e is the eroded area, and D_{n50} is the nominal diameter of the armor layer. Fig. 10 shows the reshaping of the armor rocks and the final profile of the structure. Fig. 11 depicts a DEM of the breakwater and a transversal section through the structure's center. The figure also includes a side view of the section before and after the test. Since there are so many images available, the figures were not repeated for all tests in this study.
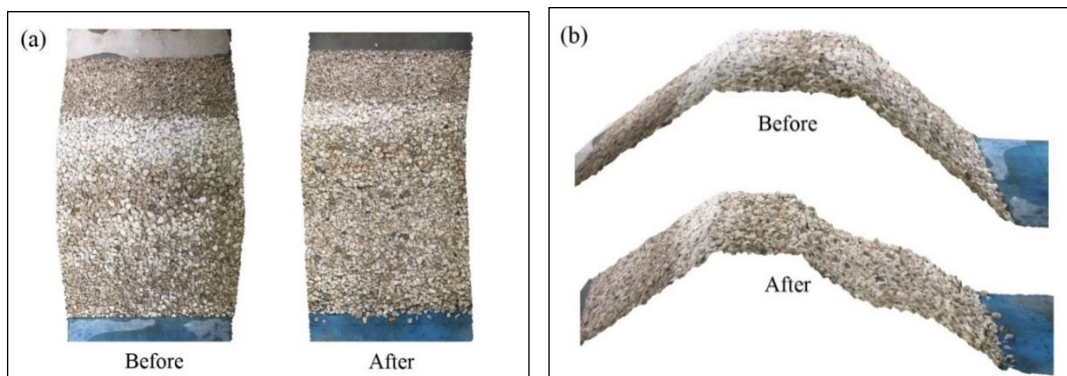

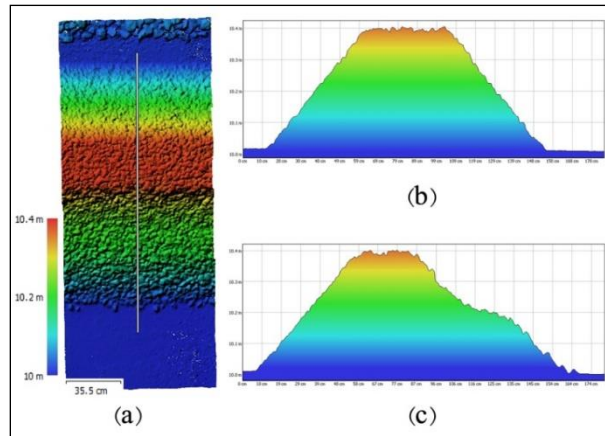**Fig. 10 - Top view and side view before and after the test**

Fig. 11 - (a) DEM and transversal section; (b) selected section before the test; (c) selected section after test

Following the tests, height, period, and the number of waves (storm duration) parameters were assessed as the primary characteristics influencing the structure's stability and monitoring the erosion when the obstacle was connected to the RMB. For studying the stability trend, the RMB was tested with several incident waves ranging from 1000 to 6000 (Fig. 12). The damage parameter was calculated by Eq. 2. For each test, as shown, the maximum profile change (over 50%) happened when the first 1000 waves hit, and the erosion of the armor layer followed an increasing trend up to 3000 waves; the erosion pace significantly decreased between 3000 and 4000 waves. It is worth noting that erosion is considered practically insignificant between 4000 and 6000 waves. Therefore, since the erosion and reshaping of the RMB profile surpassed 90% of the absolute limit (6000 waves) when 3000 waves hit the structure section, the time when 3000 waves were hit is considered the equilibrium time. After the armor layer's stones began to fall and the breakwater section was initially reshaped (1000 waves), the wall slope became milder when it came into contact with the remaining waves. Changes in profile and rock fall gradually increased surface contact and erosion in the wave energy absorption process, resulting in increased wave energy absorption and a lower reflection coefficient of the structure. The reshaped profiles are influenced by incident waves for a fixed combination of wave height and period, as shown in Fig. 12. Fig. 13 shows the variation of the damage parameter and the number of radiated waves.
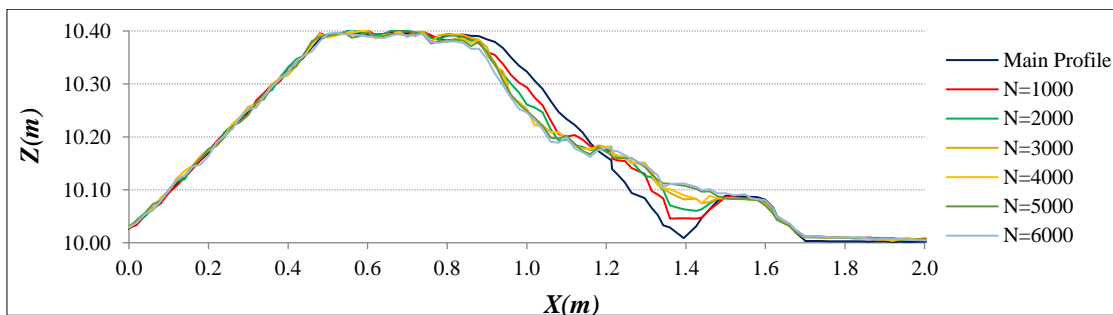

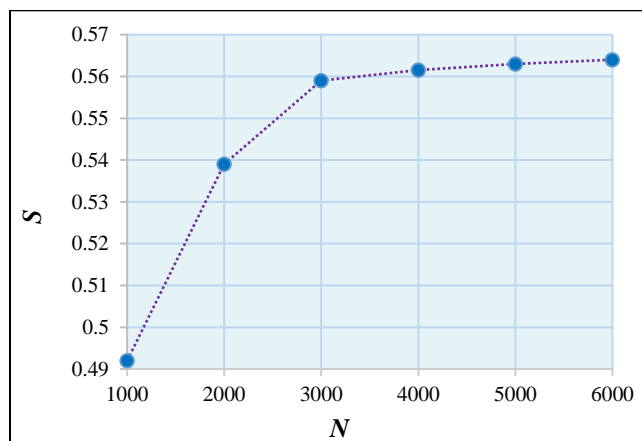**Fig. 12 - Comparison of the final profile reshaping of RMB under wave tests**

Fig. 13 - Damage parameter variations with different number of waves

Waves with a height between 9, to 15 cm were generated by a paddle towards the RMB to investigate the effect of different wave heights on the erosion rate of the structure. The erosion rate and profile reshaping were recorded (3000 waves). Fig. 14 compares the profile reshaping of RMB under different wave heights.
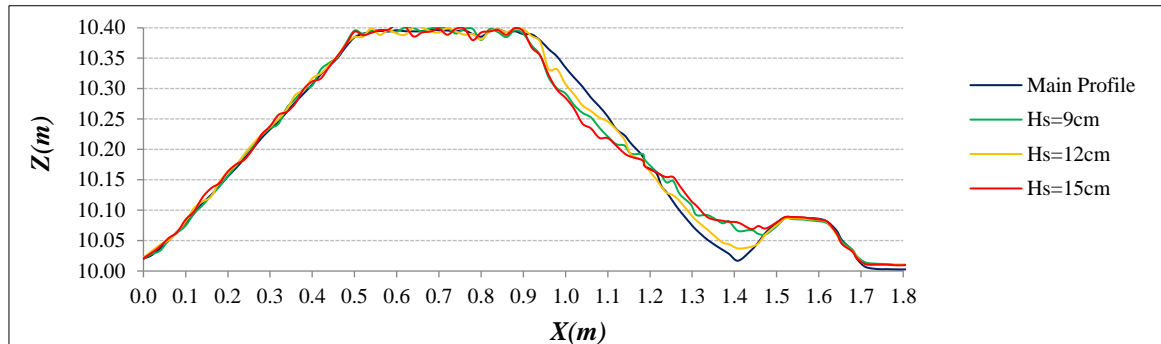

Fig. 14 - Comparison of the final profile reshaping of RMB under different wave heights

Fig. 15 plots the (non-dimensional) damage parameter against the non-dimensional wave height selected from among the numbers $\frac{H}{g.T^2}$, $\frac{H}{d}$ and $\frac{H}{H_{max}}$ (*H*: wave height, *d*: water depth, *g*: gravitational acceleration and *T*: wave period). The relationship between non-dimensional wave height and damage parameter was calculated from a linear fit as Eq. 3:

$$S = 1.936(\frac{H}{d}) - 0.363; \qquad (R^2 = 0.99) \tag{3}$$

Table 4 shows the relative wave height and damage parameter values. As shown, increasing the relative wave height from 0.36 to 0.48 and 0.6 increased the damage parameters by 39.12 and 44.44%, respectively. As well the effect of three different relative wave heights at RMB (*H/d* = 0.36, 0.48, and 0.6) on the damage parameter is indicated in Fig. 16. Since the wave energy is proportional to the square of the wave height, larger destabilizing forces would be engendered during the more considerable wave heights.
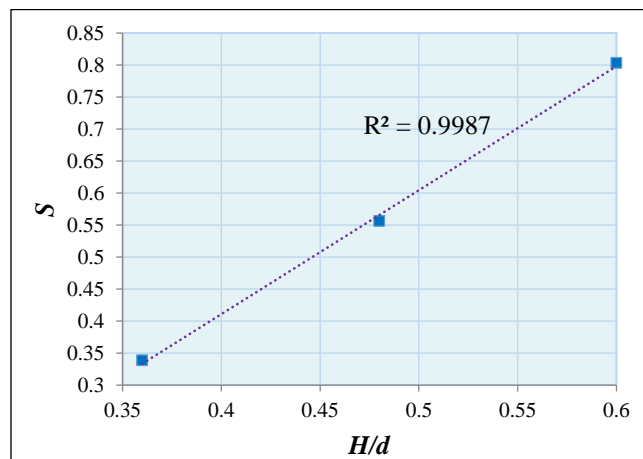

Fig. 15 - Comparison of the final profile reshaping of RMB under different wave heights

Table 4 - Non-dimensional characteristics

H /d	0.36	0.48	0.60
S	0.3384	0.5560	0.8031

According to analysis, as a parameter influencing RMB stability, the wave period demonstrated that erosion increased with an increasing wave period (Fig. 17). Table 5 shows the relative wave period numbers (period over the maximum period) and damage parameters. These figures show that as the relative wave period increased from 0.6 to 0.8 and 1, the damage parameters increased by 22.94 and 28.26%, respectively. Increasing the period would thus increase the damage parameter; however, increasing the wave height would have a significant effect. Also Fig. 18 indicates the effect of three various relative wave periods (*T_p/T_max* = 0.6, 0.8, and 1) on the damage parameter. A glance at the provided figure reveals the increasing trend in the damage parameter as the wave period increases.
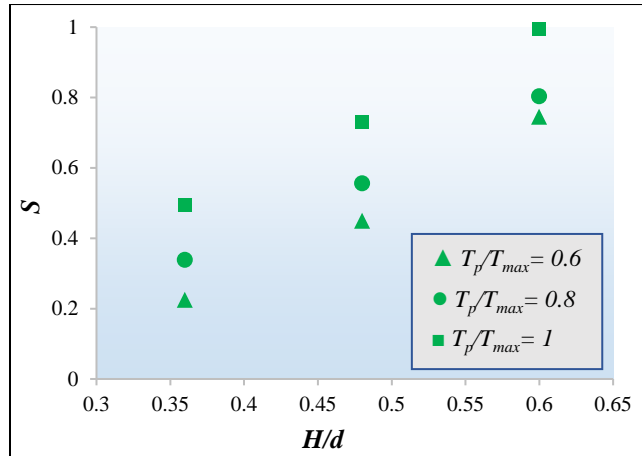
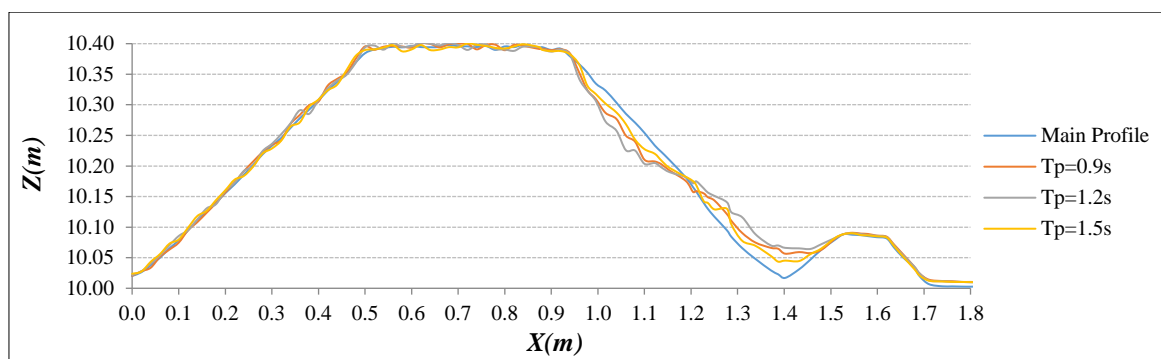**Fig. 16 - Damage parameter variations with different number of waves**

Fig. 17 - Comparison of the final profile reshaping of RMB under different wave periods

Table 5 - Relative wave period and damage parameter

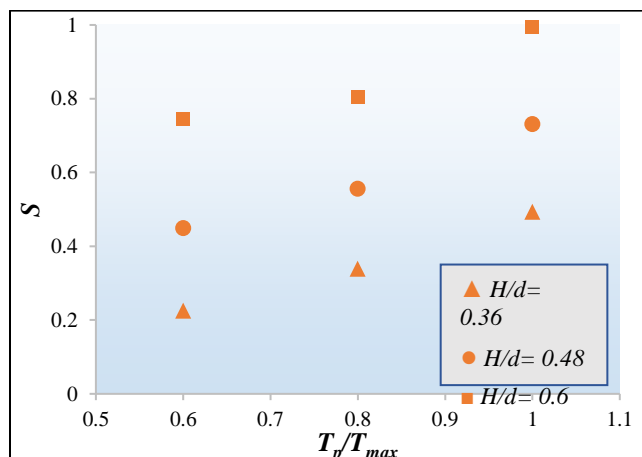| T/ T_{max}	0.6	0.8	1
S	0.4284	0.5560	0.7131

Fig. 18 - Comparison of the final profile reshaping of RMB under different wave periods

3.3 Analysis and Comparison of Strengthened Models

The distance of the reinforcing obstacle from the main breakwater is an essential and determining factor in studying the breakwater amplification by the submerged structure. Using an obstacle attached to the structure will have the same function as a berm, and placing the obstacle at a long distance will be similar to the performance of offshore breakwaters. Determining the distance between the structure and the reinforcing obstacle affects its role. As a result, in the range of zero to twenty centimeters (with a step of five centimeters), all these options (connected / short distance / long distance)

are examined compared, and the optimal performance is determined. Table 6 lists the research tests. Because the RMB with the obstacle at 5 cm produced the lowest damage parameter, the submerged obstacle and the wave barrier (RMBSF) were tested concurrently for this case.

Table 6 - Performed tests

Test	RMB arrangement modes with obstacle and wave barrier
RMB	RMB without obstacle and wave barrier
RMBS0	RMB along with the connected obstacle without wave barrier
RMBS5	RMB along with the obstacle at 5 cm without wave barrier
RMBS10	RMB along with the obstacle at 10 cm without wave barrier
RMBS15	RMB along with the obstacle at 15 cm without wave barrier
RMBS20	RMB along with the obstacle at 20 cm without wave barrier
RMBF	RMB with wave barrier at 50 cm without obstacle
RMBSF	RMB along with the obstacle at 5 cm and wave barrier at 50 cm

Fig. 19 depicts the reshaped profile of the RMB at each transversal section for the entire RMBSF experiment. The imaging results provide a 3D reshaping; additionally, the eroded area (A_e) and the damage parameter are determined by sectioning each image. Figs. 20 and 21 show a comparison of the reshaped RMB profile under all and main test conditions. Table 7 shows the calculated damage parameters in sections, height, period, and the number of waves based on the experiments. In this table, H_{wm} is the wave height defined for the wave maker, H_s, significant wave height taken from the water surface, T_{wm}, wave period specified for the wave maker, T_s, significant wave period taken from the water surface, N, the number of waves expected and N_{pr} the number of waves taken from the water surface. As shown in Table 7, the RMB's damage parameter under random waves is 1.116. As shown in the table, the highest damage parameter pertained to the 20-cm section of the wall due to the wave behavior's complexity when hitting the breakwater, and waves also causing lateral motion upon hitting the coarse armor layer rocks. Furthermore, irregular motions in the armor layer are observed due to flow turbulence in this area; thus, accurate estimation is not possible by simply studying the stability of a single breakwater section. More sections should be considered for a more accurate assessment.
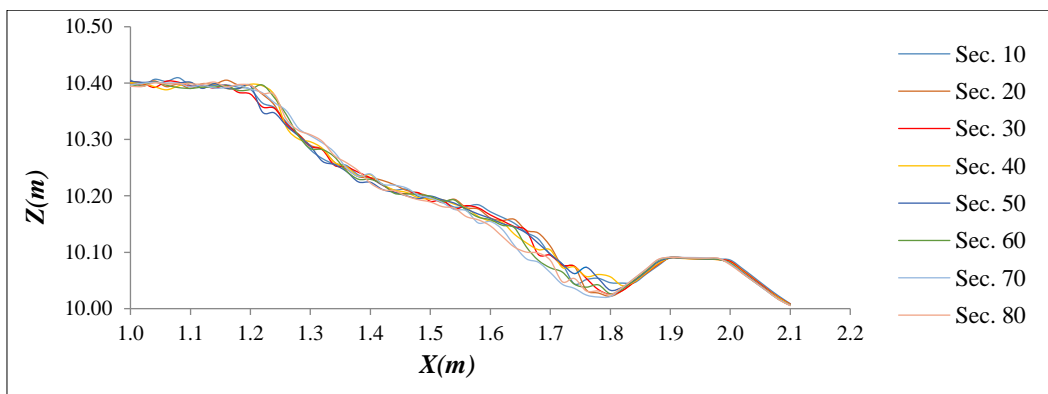

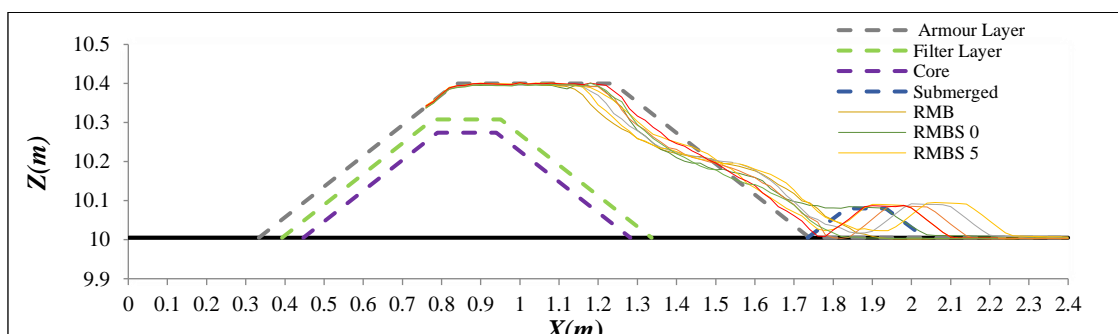**Fig. 19 - Reshaped RMB profile at each transversal section in RMBSF test**

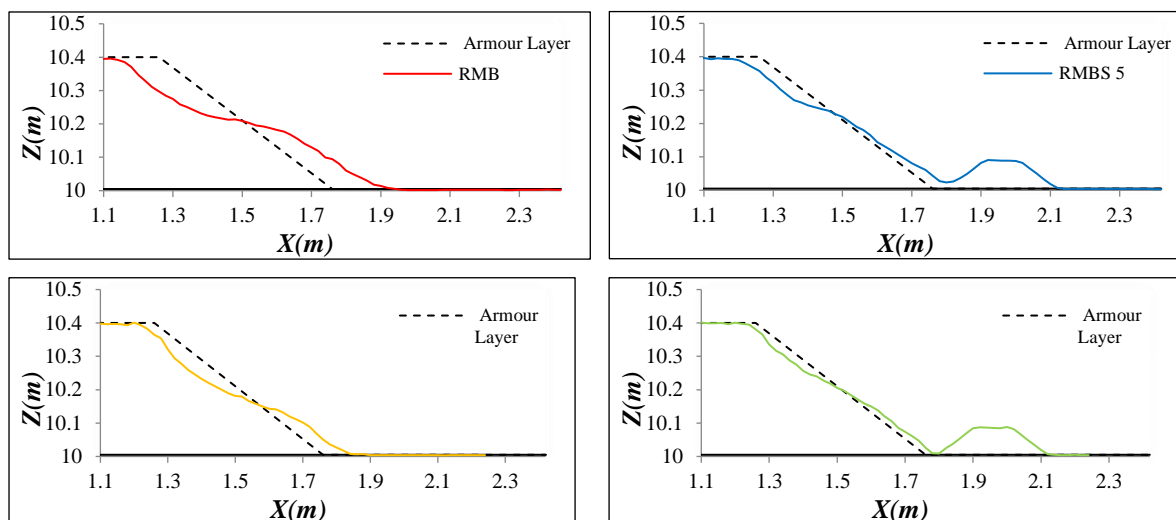**Fig. 20 - Reshaped RMB profiles in all test modes**

Fig. 21 - Comparison of reshaped RMB profiles in the main test modes

Table 7 - Damage parameter in sections, height, period, and number of waves calculated in tests

	H (cm)		T (s)		N		S									
	H_{wm}	H_s	T_{wm}	T_s	N_0	N_{pr}	S_{10}	S_{20}	S_{30}	S_{40}	S_{50}	S_{60}	S_{70}	S_{80}	S_{max}	$S_{min(Final)}$
RMB	12	11.52	1	0.95	3000	2783	1.033	1.116	1.075	1.099	1.048	1.014	1.017	0.959	1.116	
RMBS 0	12	11.29	1	0.96	3000	2593	0.626	0.574	0.572	0.701	0.699	0.698	0.660	0.516	0.701	
RMBS 5	12	11.38	1	0.98	3000	2729	0.613	0.591	0.613	0.601	0.679	0.495	0.402	0.474	0.679	
RMBS 10	12	11.63	1	0.94	3000	2801	0.517	0.541	0.583	0.591	0.768	0.647	0.630	0.471	0.768	0.513
RMBS 15	12	11.73	1	0.98	3000	2855	0.642	0.627	0.826	0.736	0.758	0.746	0.734	0.662	0.826	
RMBS 20	12	11.41	1	1.01	3000	2699	0.824	0.763	0.822	0.945	0.872	0.894	0.993	0.845	0.993	
RMBF	12	11.29	1	0.94	3000	2709	0.549	0.629	0.667	0.628	0.601	0.576	0.735	0.503	0.735	
RMBSF	12	11.59	1	0.97	3000	2787	0.479	0.464	0.423	0.463	0.450	0.513	0.413	0.458	0.513	

Installing the obstacle 5 cm from the RMB was the most effective layout, resulting in the lowest damage parameter, which was reduced by 39.15%. The wave barrier was relatively effective when placed 50 cm from the RMB, resulting in a 34.14% reduction in the damage parameter. Therefore, when used at the optimal distance, the obstacle performed better than the wave barrier. Using an optimally distanced obstacle and the wave barrier simultaneously reduced the damage parameter by 54.03%. An obstacle attached to the structure can be viewed physically as a support for the RMB, preventing it from overturning or sliding as some of the eroded rocks collide with the obstacle and come to a halt. When the obstacle is at a certain distance from the RMB, the eroded parts of the armor are poured into that gap and incorporated into the breakwater body, assisting with structural stability. The test results revealed that the distance was 5 cm. In other words, the eroded portion filling the gap was less effective at a greater distance. When a wave struck the wave barrier, it reduced the wave energy and the damage parameter accordingly. As expected, using the obstacle and wave barrier simultaneously resulted in the highest efficiency, and the reduced energy wave hit the breakwater with an obstacle at an optimal distance. It was concluded that a 54.03% reduction in the damage parameter would reduce breakwater dimensions, resulting in significant cost savings.

As shown in table 7 and Fig. 22, applying the obstacle reduced the damage parameter to 0.679 (i.e., 39.15%), whereas the wave barrier reduced the damage parameter to 0.735 (i.e., 34.14%). Thus, the obstacle has outperformed the wave barrier. Using the obstacle with the wave barrier reduced the damage parameter by 54.03%. Physically, it can be assumed that support was established for the breakwater when using the obstacle attached to the structure, which was effective against slides and overturning, with some of the eroded segments hitting it and stopping there. The use of the obstacle and the wave barrier simultaneously results in the highest efficiency, with the reduced-energy wave colliding with the existing RMB. A 54.03% reduction in damage appears to reduce RMB dimensions, significantly lowering costs.
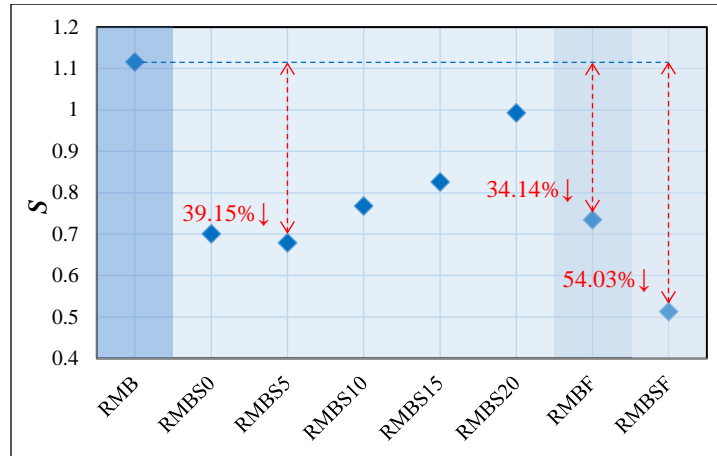
Fig. 22 - Damage parameter in all test modes and damage parameter reduction (%)

It is also appropriate to study the interaction of wave steepness (S_{op}) and the damage parameter in testing different models. This parameter is discussed in Fig. 23 according to the conditions in the reinforced model test by the obstacle and floating barrier.
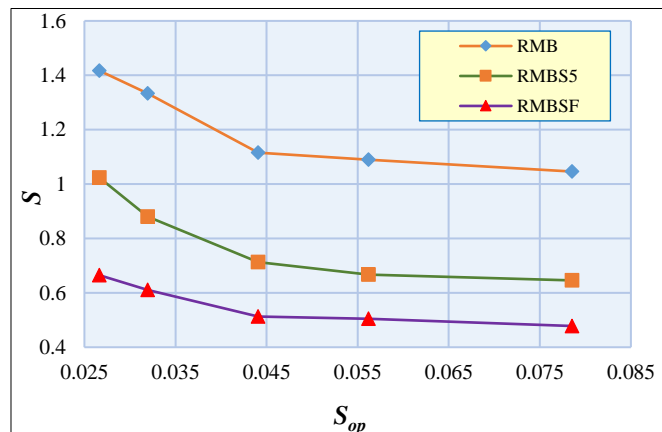

Fig. 23 - Comparison of damage parameter between experiment results with the wave steepness

4. Conclusion

Using a submerged obstacle in front of the main structure to protect against the waves' intense effect can be considered a suitable and effective method. The performance of the tandem breakwater has shown that the submerged structure significantly reduces the wave load on the main structure. According to this, the effects of a submerged obstacle and a floating wave barrier on the damage parameter of an RMB were investigated in this study. The following are the conclusions about the optimal distance of the obstacle combined with the wave barrier to reduce the damage parameter:

• Calculation of damage parameter, recording of structural behavior, and amount of deformation were performed by constructing an integrated 3D RMB model with high accuracy and reliability by the close-range photogrammetric method.

• The majority (over 50%) of the breakwater profile transformation was discovered to occur during the first 1000 wave hits. The armor layer continued to erode by up to 3000 waves, after which the erosion decreased dramatically until 4000 hits. Later, between 4000 and 6000 wave hits, erosion was negligible. As a result, the first 3000 wave hits account for 90% of the RMB's final erosion and profile transformation. As well, increasing the wave height increased the damage parameter; increasing the relative wave height from 0.36 to 0.48 and then to 0.6 increased the damage parameter by 39.12 and 44.44%, respectively. Also, the damage parameter increased with longer periods. Increasing the relative wave period from 0.6 to 0.8 and then to 1 increased the damage parameter by 22.94 and 28.26%, respectively.

• According to the test results, different levels of damage vary recorded at different cross-sections. According to this, the middle band cannot be recommended for a stability study. Having both DEM and DSM, different damage sections was examined.

• The damage parameter was calculated at 1.116 in tests with models of the RMB without obstacles exposed to random waves. Using a connected obstacle reduced the damage parameter to 0.701, and the damage parameter was calculated at 5, 10, 15, and 20 cm distances to be 0.679, 0.768, 0.826, and 0.993, respectively. The tests revealed that at

5 cm, spacing between the submerged obstacle and the RMB was the most effective in lowering the damage parameter by 39.15%. Accordingly, a 5 cm distance was proposed between the submerged obstacle and the RMB.

• Placing the floating wave barrier 50 cm away from the (seaward) RMB reduced the height and energy of the waves impinging on the breakwater, resulting in less structural damage. Accordingly, the best results were obtained by spacing the obstacle and the RMB by 5 cm and placing the wave barrier at a distance of 50 cm (eq. to 54.03%). These distances were effective in reducing wave energy and controlling damage to the RMB. Lower damage parameters can also significantly reduce RMB dimensions and, as a result, associated costs.

• The study of the interaction between the wave steepness and the damage parameter showed that the damage decreases with increasing wave steepness values.

Abbreviations and Symbols

Abbreviations		T_p	Peak wave period
RMB	Rubble mound breakwater	N	Storm duration (number of waves)
RMBS	Rubble mound breakwater with submerged obstacle	d	Water depth
		D_{n50}	Armor material nominal diameter (cm)
RMBF	Rubble mound breakwater with floating wave barrier	X	Location of submerged obstacle (cm)
		H/d	Relative wave height
RMBSF	Rubble mound breakwater with submerged obstacle and floating wave barrier	T/T_{max}	Relative wave period
		s_{om}	Steepness parameter
DEM	Digital elevation model	A_e	Eroded area
DSM	Digital surface model	S	Damage parameter
FSI	Fluid-structure interaction	H_{wm}	Wave height defined for the wave maker (cm)
PCR	Principal component regression	H_s	significant wave height (cm)
SCWMRI	Soil conservation and watershed management research institute	T_{wm}	wave period defined for the wave maker (s)
		T_s	significant wave period (s)
List of symbols		N_{pr}	the number of waves taken from the water surface
g	acceleration of gravity	H_0	stability number
f_g	gradation factor of armor stones	T_0	wave period inde
ρ	Mass density	H_0T_0	period stability numbe
$cot\ \alpha$	front slop	R_e	Reynolds number for armor stone
υ	kinematic viscosity	S_o	mean wave steepnes

Acknowledgement

References

Andersen, T. L. (2006). *Hydraulic Response of Rubble Mound Breakwaters: Scale Effects - Berm Breakwaters.* Hydraulics & Coastal Engineering Laboratory, Department of Civil Engineering Aalborg University: Ph.D. Thesis, Series paper No. 27.

Ataie Ashtiani, B. (2006). *Coastal Engineering (Coastal Hydrodynamics)*. Tehran: ACECR, Amirkabir University of Technology Branch. pp. 214-218

Bungin, E. R. (2021). The effect of square submerged breakwater on wave transmission in the coastal area. *AC2SET (2020), IOP Conference series: Materials Science and Engineering*. Medan, Indonesia. September 2020: 1088 012099.

Burcharth, H. F. (1993). *Design of Breakwaters.* Department of Civil Engineering, Department of Civil Engineering Aalborg University: Ph.D. Thesis.

Campos, A., Castillo, C. & Sanchez, R. (2020). Damage in rubble mound breakwaters. Part I: Historical review of damage models. *Journal of Marine Science and Engineering,* 8. 317, from doi: 10.3390/jmse8050317

Celli, D., Li, Y., Ong, M. C. & Di Risio, M. (2019). The role of submerged berms on the momentary liquefaction around conventional rubble mound breakwaters. *Applied Ocean Research*, 85. pp. 1-11, from doi: 10.1016/j.apor.2019.01.023

Celli, D., Pasquali, D., Girolamo, P. & Di Risio, M. (2018). Effects of submerged berms on the stability of conventional rubble mound breakwaters. *Coastal Engineering*, 136. pp. 16-25, from doi: 10.1016/j.coastaleng.2018.01.011

Chegini, V. (2010). *Design Principles of Coastal Structures.* Tehran. Iranian National Institute for Oceanography.

Cox, J. C. & Clark, G. R. (1992). Design and development of a tandem breakwater system for Hammond Indiana. *Coastal Structures and Breakwaters.* London: Thomas Telford, pp. 111–121.

Da Silva, R. F., Sayao, O. & Conceicao, L. P. (2016). Analysis of rubble mound breakwater damage: Case study of existing breakwater rehabilitation. *IX Pinac Copedec Conference*. Rio de Janeiro, Brazil. January 2016.

Ebadi, H. & Esmaeili, F. (2018). *Applications of 3D Measurement of Images.* Tehran: Khajeh Nasir Toosi University of Technology (KNTU).

Galiatsatou, P., Makris, C. & Prinos, P. (2018). Optimized reliability based upgrading of rubble mound breakwaters in a changing climate. *Journal of Marine Science and Engineering*. 6(3). 92, from doi: 10.3390/jmse6030092

Ghanbarian, M. (2010*). Rubble mound breakwaters (Vol.1: Types of breakwaters, principles, and overview).* Tehran: Khatam-al-Anbiya Construction Headquarter. pp. 15-19.

Hao, Q., Lin, M., Wenyong, T. & Zhe, H. (2019). Numerical study of the interaction between peregrine breather based freak waves and twin-plate breakwater. *Journal of Fluids and Structures*. 87. pp. 206-227, from doi: 10.1016/j.jfluidstructs.2019.04.003

Hughes, S. A. (1993). *Physical models and laboratory techniques in coastal engineering. Advanced Series on Ocean Engineering. Vol. 7.* New Jersey: World Scientific.

Janardhan, P., Harish, N., Rao, S. & Shirlal, K. G. (2015). Performance of variable selection method for the damage level prediction of reshaped berm breakwater. *International Conference on Water Resources, Coastal and Ocean Engineering (ICWRCOE 2015).* Kozhikode, India. December 2015. pp. 302- 307

Jensen, O. J. & Klinting, P. (1983). Evaluation of scale effects in hydraulic models by analysis of laminar and turbulent flow. *Coastal. Engineering.* 7, pp. 319–329

Juhl, J. & Jensen, O. J. (1995). Features of berm breakwaters and practical experience. *Proceeding of the International Conference on Coastal and Port Engineering in Developing Countries.* R.J. Brazil. September 25-29, 1995. pp. 1307-1320

Khosravi Babadi, M., Golshani, A., Ghanei Ardakani, A. & Karami Matin, A. (2017). *Design principles of breakwaters.* Tehran: Marine Industries Organization Publication.

Lamberti, A., Tomasicchio, G. R. & Guiducci, F. (1994). Reshaping breakwaters in deep and shallow water conditions. *Proceeding of 24ᵗʰ International Conference on Coastal Engineering.* Kobe, Japan. October 23-28, 1994. ASCE pp. 1343-1358

Mostaghiman, A. & Moghim, M. (2022). An experimental study of partly/hardly reshaping mass-armored double-berm breakwaters. *Ocean Engineering*. 243, 110258, from doi: 10.1016/j.oceaneng.2021.110258

Mousavi, S. H. (2010). *Rubble mound breakwaters (Vol.2: Design of rubble mound breakwaters).* Tehran: Khatam-al-Anbiya Construction Headquarter Publication.

Neves, A., Veloso-Gomes, F. & Taveira-Pinto, F. (2007). Analysis of the wave-flow interaction with submerged breakwaters. *WIT Transactions on Modelling and Simulation*. 46. pp. 147-154, from doi: 10.2495/CMEM070151

Padashi, Y., Tajziyehchi, M. (2010). Study of wave breaking type effect on current passing over submerged breakwaters and reefs. *International Conference on Coasts, Ports and Marine Structures (ICOPMAS).* Iran.Tehran. November 29- December 1, 2010.

Rao, S., Pramod, C. h. & Rao, B. (2004). Stability of berm breakwater with reduced armor stone weight. *Ocean Engineering*. 31. pp. 1577–1589, from doi: 10.1016/j.oceaneng.2003.12.010

Sayao, O. (1998). On the profile reshaping of berm breakwaters. *Coastal structures.* 99. pp. 224-265

Smith, D. A. Y., Warner, P. S. & Sorensen, R. M. (1996). *Submerged-crest breakwater design. Advances in Coastal Structures and Breakwaters.* London: Thomas Telford. pp. 208–219

Stefanutti Stocks Marine (2015) *Rubble mound breakwater vs. tandem breakwater cost estimation.* Johannesburg: Stefanutti Stocks Holding Limited.

Tulsi, K. & Phelp, D. (2009). Monitoring and maintenance of breakwaters which protect port entrances. *28th Annual Transport Conference (SATC) 2009.* Pretoria, South Africa. July 6-9 2009. pp.317 – 325

Vafaeipour Sorkhabi, R. & Naseri, A. (2019). Experimental investigation of the interaction between vertical flexible seawall and random sea waves. *Journal of Advanced Defense Science and Technology.* 6(3), pp. 155-162

Van der Meer, J. W. (1992). *Conceptual design of rubble mound breakwaters.* Delft Hydraulics, Delft, Netherlands. Report No. 483. TLJ7000. Oct. 01, 1992

Van der Meer, J. W. (1988). *Rock slopes and gravel beaches under wave attack.* Delft University of Technology: Ph.D. Thesis. Delft Hydraulics Communication. No. 396.

Van Gent, R. A. (2013). Rock stability of rubble mound breakwaters with a berm. *Coastal Engineering*. 78. pp. 35-45, from doi: 10.1016/j.coastaleng.2013.03.003

Van Gent, R.A. & Van der Werf, M, (2014), Rock toe stability of rubble mound breakwaters. *Coastal Engineering*. 83. pp. 166-176, from doi: 10.1016/j.coastaleng.2013.10.012

Vidal, C., Medina, R. & Lomonaco, P. (2006). Wave height parameter for damage description of rubble-mound breakwaters. *Coastal Engineering*. 53. pp. 711-722, from doi: 10.1016/j.coastaleng.2006.02.007

Viriyakijja, K. & Chinnarasri, C. (2015). Wave flume measurement using image analysis. *Aquatic Procedia.* Elsevier. 4. pp. 522-531, from doi: 10.1016/j.aqpro.2015.02.068